The Binding of the PDZ Tandem of Syntenin to Target Proteins[†,‡]

Jolanta Grembecka,[§,||] Tomasz Cierpicki,[§,⊥] Yancho Devedjiev,[§] Urszula Derewenda,[§] Beom Sik Kang,[#] John H. Bushweller,[§] and Zygmunt S. Derewenda*[,§]

Department of Molecular Physiology and Biological Physics, University of Virginia School of Medicine, Charlottesville, Virginia 22908-0736, and School of Life Science & Biotechnology, Kyungpook National University, Daegu 702-701, Korea

Received November 1, 2005; Revised Manuscript Received January 18, 2006

ABSTRACT: PDZ domains are among the most abundant protein modules in the known genomes. Their main function is to provide scaffolds for membrane-associated protein complexes by binding to the cytosolic, C-terminal fragments of receptors, channels, and other integral membrane proteins. Here, using both heteronuclear NMR and single crystal X-ray diffraction, we show how peptides with different sequences, including those corresponding to the C-termini of syndecan, neurexin, and ephrin B, can simultaneously bind to both PDZ domains of the scaffolding protein syntenin. The PDZ2 domain binds these peptides in the canonical fashion, and an induced fit mechanism allows for the accommodation of a range of side chains in the P_0 and P_{-2} positions. However, binding to the PDZ1 domain requires that the target peptide assume a noncanonical conformation. These data help explain how syntenin, and perhaps other PDZ-containing proteins, may preferentially bind to dimeric and clustered targets, and provide a mechanistic explanation for the previously reported cooperative ligand binding by syntenin's two PDZ domains.

PDZ[1] domains (postsynaptic density protein, disc large, and zonula occludens) are found in all organisms from bacteria to vertebrates and constitute one of the most abundant protein domain families in the human genome (*1*, *2*). These protein modules are found within diverse, multidomain regulatory cytoplasmic proteins and play an important role in their targeting to specific cell membrane receptors and channels and in assembling supramolecular signaling complexes (*3*). The PDZ domains are approximately 90 residues long and are structurally highly conserved in spite of significant sequence diversity (*4*). They function by binding to the C-terminal fragments of target proteins with the terminal carboxylate anchored within a unique, glycine-rich loop (*4*). The bound fragment typically assumes an extended conformation, and the canonical model of the PDZ−target interaction implies that the selectivity is accomplished primarily by the side chains of residues P_0 and P_{-2}, both of which fitting into their respective specificity pockets (*5*). However, this model fails to explain the diversity of the observed interactions, including degeneracy of specificity and apparent cooperativity of binding of certain PDZ-containing proteins to their oligomeric targets (*6*).

Syntenin is an adaptor-like molecule containing two PDZ domains (*7*). It was originally identified as a syndecan binding protein (*8*) and subsequently found to be involved in diverse physiological processes such as cell adhesion (*9*), protein trafficking (*10*, *11*), and activation of transcription factors (*12*). Syntenin was found to be overexpressed in breast and gastric cancer cells promoting their migration and metastasis (*13*). The diverse biological functions of syntenin result from its binding to the cytoplasmic domains of numerous physiologically relevant signaling and adhesion molecules, such as syndecans (*8*, *14*), neurexins (*14*, *15*), and ephrin B (*14*, *16*, *17*), among others. Since these targets contain diverse C-terminal sequences, syntenin must exhibit considerable degeneracy of specificity. It has also been established by several independent studies that interactions of syntenin with cell-surface proteins are mediated cooperatively by both of its PDZ domains (*8*, *10*, *14*−*16*), suggesting that at least in some cases the two distinctly different PDZ domains bind identical target sequences.

Mutational (*8*, *14*) and crystallographic studies (*7*) provided some insight into the molecular mechanism of syntenin and revealed that syntenin mainly recognizes the side chains of the three C-terminal amino acids in the target protein (P_0, P_{-1}, and P_{-2}) while the residues upstream are not involved. The combinatorial utilization of any two of the three pockets in the PDZ2 domain provides some explanation of degenerate specificities, but neither for the cooperative effects nor for the synergistic binding of both PDZ domains to the same target (*18*). In order to better understand these phenomena, we designed a series of peptides containing the C-terminal

[†] This work was supported by DOD Grant DAMD17-01-1-0720 to Z.S.D.

[‡] Structure coordinates have been deposited in the PDB with ID codes 1V1T, 1W9E, 1W9O, and 1YBO for the complexes of syntenin tandem with TNEYKV, TNEFYF, TNEYYV, and syndecan 17-mer, respectively.

* Author to whom correspondence should be addressed. E-mail: zsd4n@virginia.edu. Tel: (434) 924 5108. Fax: (434) 982 1616.

[§] University of Virginia School of Medicine.

[||] On leave from the Wroclaw University of Technology, Poland.

[⊥] On leave from the University of Wroclaw, Poland.

[#] Kyungpook National University.

[1] Abbreviations: PDZ, postsynaptic density protein, disc large, and zonula occludens); PEG, poly(ethylene glycol); HSQC, heteronuclear single quantum coherence; ITC, isothermal titration calorimetry; GRIP1, glucocorticoid receptor interacting protein 1; Pals1, protein associated with lin seven-1; Par6, partitioning-defective protein 6; NHERF, sodium−hydrogen exchanger regulatory factor; PSD-95, postsynaptic density protein of 95 kDa.

10.1021/bi052225y CCC: $33.50
Published on Web 02/21/2006

tripeptide sequences corresponding to, among others, syndecan, neurexin, and ephrin B, and we studied their interactions with the intact PDZ tandem of syntenin in solution, using heteronuclear NMR spectroscopy, as well as in crystals, using crystallography.

Our results confirm that peptides corresponding to the C-termini of selected cell-surface proteins can simultaneously interact with both PDZ1 and PDZ2 domains of syntenin, although with markedly different affinities. The crystal structures of the PDZ tandem in complex with four different peptides confirm the canonical model of peptide recognition by the PDZ2 module. Further, we extend our model for degenerate binding through description of an induced fit mechanism by which the PDZ2 binding groove adapts conformationally to diverse sequences. We also present NMR and crystallographic evidence for noncanonical interactions of the PDZ1 domain with peptide targets. These data help to understand syntenin's interactions with its targets and suggest a possible explanation for the previously reported cooperative effects.

MATERIALS AND METHODS

Design of Peptides. Because of the apparent discrepancy between the original report of the cooperative binding of both PDZ domains of syntenin to syndecan (*8*, *14*) and our previously reported work which showed that the isolated PDZ2 domain binds the syndecan derived peptide in a manner similar to that of the tandem (*7*), we first investigated the binding of the syndecan's C-terminal 17-mer peptide to the intact PDZ tandem of syntenin using X-ray diffraction. The refined model revealed a peptide ligand bound only to PDZ2 of both molecules in the asymmetric unit. Out of the 17 amino acids of the peptide, only six were visible in the electron density map bound to the PDZ2 domain of molecule 1, and just four in molecule 2. No side chains upstream of P_{-2} were engaged in the interactions. Interestingly, the critical intermolecular contacts in this crystal were formed by the glutamate in the P_{-3} position of the peptide, and not by the protein. This suggested to us that we could use the syndecan template (TNEFYA) to generate a series of isomorphous crystal complexes with varying C-terminal tripeptides. Such isomorphous series gave us the opportunity to study in some detail any potential induced-fit effects. Consequently, we used hexapeptides with the sequences TNE**YYV** (where YYV corresponds to the C-terminus of neurexin), TNE**YKV** (where YKV is the signature sequence for ephrin B), and a synthetic peptide TNE**FYF** designed for optimal fit into the PDZ2 pocket. The use of such hexapeptides as models for ephrin and neurexin C-termini is justified by mutational (*8*, *14*) and crystallographic studies (*7*), which revealed that syntenin mainly recognizes the three C-terminal amino acids in the target protein (P_0, P_{-1}, and P_{-2}) while the residues upstream are not involved. We also used the syndecan wild-type TNEFYA hexapeptide for binding measurements, to complete the series.

Protein Expression, Purification, and Crystallization. A syntenin PDZ tandem (residues 113−273) was expressed and purified according to the procedures described elsewhere (*7*). Synthesized peptides syndecan 17-mer, TNEFYF, TNEYYV, and TNEYKV were purchased from BioSynthesis, Inc. An initial search for crystals of complexes of syntenin PDZ tandem with peptides was carried out with the PEG Ion Crystal screen (Hampton Research). The best crystals were obtained with 8 mg/mL protein concentration, from 0.2 M NH_4Cl and 20% PEG 3350, using a 1:4 molar ratio of protein and peptide. Drops were formed with 1 μL of protein solution and 1 μL of reservoir solution and were overlaid with 15 μL of a 1:1 mixture of silicon and mineral oil. The best crystals were obtained by microseeding using the sitting drop vapor-diffusion technique at room temperature.

Table 1: Crystallographic Data

data set	TNEFYF	TNEYYV	TNEYKV	syndecan 17-mer
Experimental Data				
wavelength (λ)	0.97946	1.04020	0.97912	0.97960
space group	$P4_12_12$	$P4_12_12$	$P4_12_12$	$P4_12_12$
unit cell params (Å)				
a	72.21	72.13	73.34	73.32
b	72.21	72.13	73.34	73.32
c	126.05	126.22	125.68	125.92
resolution (Å)	63.25−1.56 (1.63−1.56)[a]	50.0−2.25 (2.33−2.25)	63.25−1.75 (1.81−1.75)	40.0−2.3 (2.38−2.3)
unique reflns	48061	16413	34079	15450
completeness (%)	100	99.2 (99.4)	98.7 (99.8)	99.3 (99.9)
R_{merge} (%)[b]	6.3 (52.5)	6.6 (35.6)	9.1 (26.2)	6.1 (12.6)
average $I/\sigma(I)$	39.9 (4.25)	29.3 (6.4)	19.0 (5.7)	30.9 (18.4)
Refinement Details				
resolution (Å)	63.25−1.56	8.0−2.25	63.25−1.80	40.0−2.3
reflns (working)	47197	15024	30277	14591
reflns (test)	989	945	993	800
R_{work} (%)[c]	17.2	21.8	18.3	19.3
R_{free} (%)[c]	20.1	28.1	22.9	27.4
no. of waters	395	200	281	190
Rms Deviation from Ideal Geometry				
bonds (Å)	0.017	0.011	0.016	0.011
angles (deg)	1.494	1.200	1.475	2.612
average *B* factor (Å^2)				
main chain	19.6	31.5	28.8	27.7
side chain	23.2	32.7	32.5	28.3
waters	39.9	42.7	44.5	31.9
peptide in PDZ2	29.4	41.6	37.0	34.6
peptide in PDZ1	33.8			

[a] The numbers in parentheses describe the relevant value for the highest resolution shell. [b] $R_{merge} = \sum|I_i - \langle I\rangle|/\sum I$, where I_i is the intensity of the *i*th observation and $\langle I\rangle$ is the mean intensity of the reflections. [c] $R = \sum||F_o| - |F_c||/\sum|F_o|$, crystallographic *R* factor, and $R_{free} = \sum||F_o| - |F_c||/\sum|F_o|$, where all reflections belong to the test set of randomly selected data.

Data Collection, Structure Determination, and Refinement. Crystals used for data collection were briefly soaked in the crystallization buffer containing 15% glycerol and frozen by immersion in liquid nitrogen. Data for the complex with TNEFYF, TNEYYV, and syndecan 17-mer peptides were collected at beamline X9B at the National Synchrotron Light Source (Brookhaven National Laboratory) under cryoconditions using the ADSC Quantum4 CCD detector. Data for the complex with TNEYKV were collected at beamline 22ID at the Advanced Photon Source (Argonne National Laboratory), also under cryoconditions and with the MAR-RESEARCH CCD detector. Data were processed and scaled using HKL2000 (*19*). Crystallographic details, including unit cells and data statistics, are shown in Table 1. The positions of the starting models for the PDZ tandem molecules were optimized using AMORE (*20*). As a search model for the complex of the syntenin PDZ tandem with the TNEFYF peptide we used the structure of the unliganded PDZ tandem (entry 1N99 in the PDB). Subsequently, the complex with TNEFYF peptide refined at 1.56 Å resolution was used as a

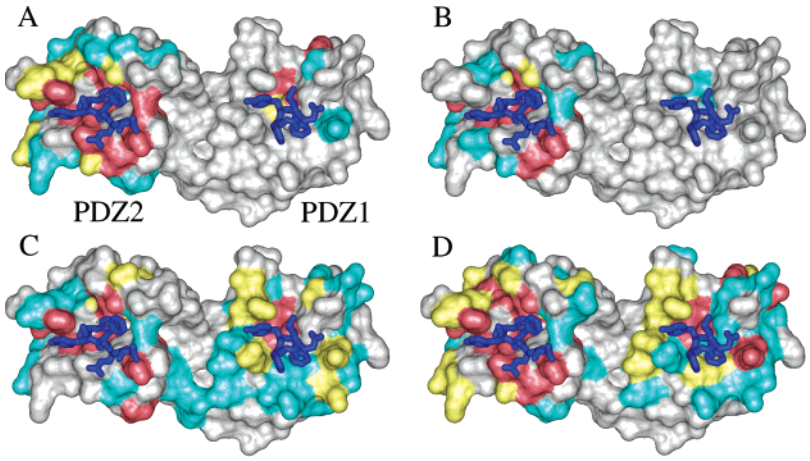

FIGURE 1: Chemical shift changes of amides observed upon titration of the syntenin PDZ tandem with hexapeptides: (A) TNEFYA; (B) TNEYKV; (C) TNEFYF; (D) TNEYYV. Chemical shift changes are mapped onto the structure of the complex with the TNEFYF peptide (peptides in PDZ1 and PDZ2 are shown in blue). Color coding is based on the magnitude of chemical shift perturbation (Δ) calculated according to the formula $\Delta = [\Delta\sigma_{HN}^2 + (0.11\Delta\sigma_N)^2]^{1/2}$. The following colors are used: gray, $\Delta < 0.05$ ppm; cyan, $0.05 \leq \Delta < 0.1$ ppm; yellow, $\Delta \geq 0.1$ ppm; the most perturbed amides broadened beyond the detection limit upon complex formation are shown in red.

starting model for the molecular replacement. The atomic models were refined with REFMAC5 (*21*) from the CCP4 suite (*22*). The structures were refined to 1.56 Å, 1.8 Å, 2.25 Å, and 2.3 Å for the complex of syntenin PDZ tandem with TNEFYF, TNEYKV, TNEYYV, and syndecan 17-mer peptides. Manual model building was performed in O (*23*). The details of the refinement are given in Table 1.

NMR Measurements. Measurements of syntenin−peptide interactions were carried out using a series of ^{1}H−^{15}N HSQC spectra. Experiments were carried out using 0.2 mM ^{15}N labeled PDZ tandem (residues 113−273) in 50 mM phosphate buffer, pH 6.5 and 150 mM NaCl at 30 °C. Samples for titration experiments were prepared by mixing 0.2 mM protein with 20 mM peptide stock solutions (in DMSO-d_6) in ratios ranging from 1:0.5 to 1:16. Dissociation constants for syntenin−peptide complexes were calculated from least-squares fitting of chemical shift changes as a function of ligand concentration (*24*). Interpretation of chemical shift changes was based on previously completed assignment (*25*). NMR spectra were collected at 30 °C using Varian Inova 500 and 600 MHz spectrometers. Processing and analysis of NMR spectra was carried out in NMRPipe (*26*) and Sparky (Goddard, T. D., and Kneller, J. M., University of California, San Francisco) programs.

RESULTS

Binding of Target Peptides to PDZ Domains of Syntenin in Solution. In order to evaluate the binding of the designed hexapeptides to the PDZ tandem we used heteronuclear NMR spectroscopy. In contrast to other techniques, analysis of chemical shift perturbation allows for both the detection of low affinity interactions and the detection of independent binding to each of the two PDZ domains within the tandem. We first carried out the assignment of ^{1}H and ^{15}N chemical shifts for the ^{15}N-labeled tandem, residues 113−273 (*25*). The binding was analyzed using a series of ^{1}H−^{15}N HSQC spectra recorded for the PDZ tandem in the presence of peptides at increasing concentrations. The data unambiguously identified the residues affected by peptide binding and yielded dissociation constants from the fitting of chemical shift changes as a function of a ligand concentration (*24*). Figure 1 shows the PDZ tandem of syntenin with residues color coded for chemical shifts observed upon titration with TNEFYA (Figure 1A), TNEYKV (Figure 1B), TNEFYF (Figure 1C), and TNEYYV (Figure 1D) peptides. All peptides bind to both PDZ1 and PDZ2 (see also Figure 2A), although the magnitudes of the associated chemical shift changes differ significantly. Data are consistent with fast exchange kinetics (Figure 2B−D) and relatively weak affinities (Table 2). In all cases the most significant chemical shift changes are seen within the PDZ2 domain, with corresponding dissociation constant (K_D) values within a 0.1−1.15 mM range. The TNEFYF and TNEYYV (neurexin) peptides also cause extensive chemical shift perturbations in the PDZ1 domain, consistent with similar affinities. In contrast, the TNEFYA (syndecan) and TNEYKV (ephrin B) peptides bind to PDZ1 poorly, with K_D values higher by least an order of magnitude.

Crystal Structures of Peptide−Tandem Complexes: Quality of Atomic Models. Structures of the PDZ tandem with the TNEYYV, TNEYKV, and TNEFYF hexapeptides were refined at 2.25 Å, 1.80 Å and 1.56 Å, respectively (Table 1). The corresponding atomic models were refined to crystallographic R factor values of 21.8% (R_{free} = 28.1%), 18.3% (R_{free} = 22.9%), and 17.2% (R_{free} = 20.1%). In each case the asymmetric unit contained a noncrystallographic dimer of PDZ tandems (residues 113−273 of syntenin). With the exceptions of no more than five side chains per tandem, all residues were clearly visible in the σ_A-weighted $2mF_o - DF_c$ electron density map contoured at 1σ. The average temperature factors (B) for main chain atoms were: 19.6, 31.5, and 28.8 Å^2 for the complexes with TNEFYF, TNEYYV, and TNEYKV (Table 1). In all complexes, peptides were found in the binding grooves of both PDZ2 domains within the noncrystallographic dimer (Figure 3B−D). With the exception of the complex involving the TNEFYF peptide, no interpretable electron density was observed in the PDZ1 binding groove. However, there was unambiguously interpretable electron density for the four C-terminal amino acids of the TNEFYF peptide in the binding groove of the PDZ1 domain of molecule 1 (Figure 3A).

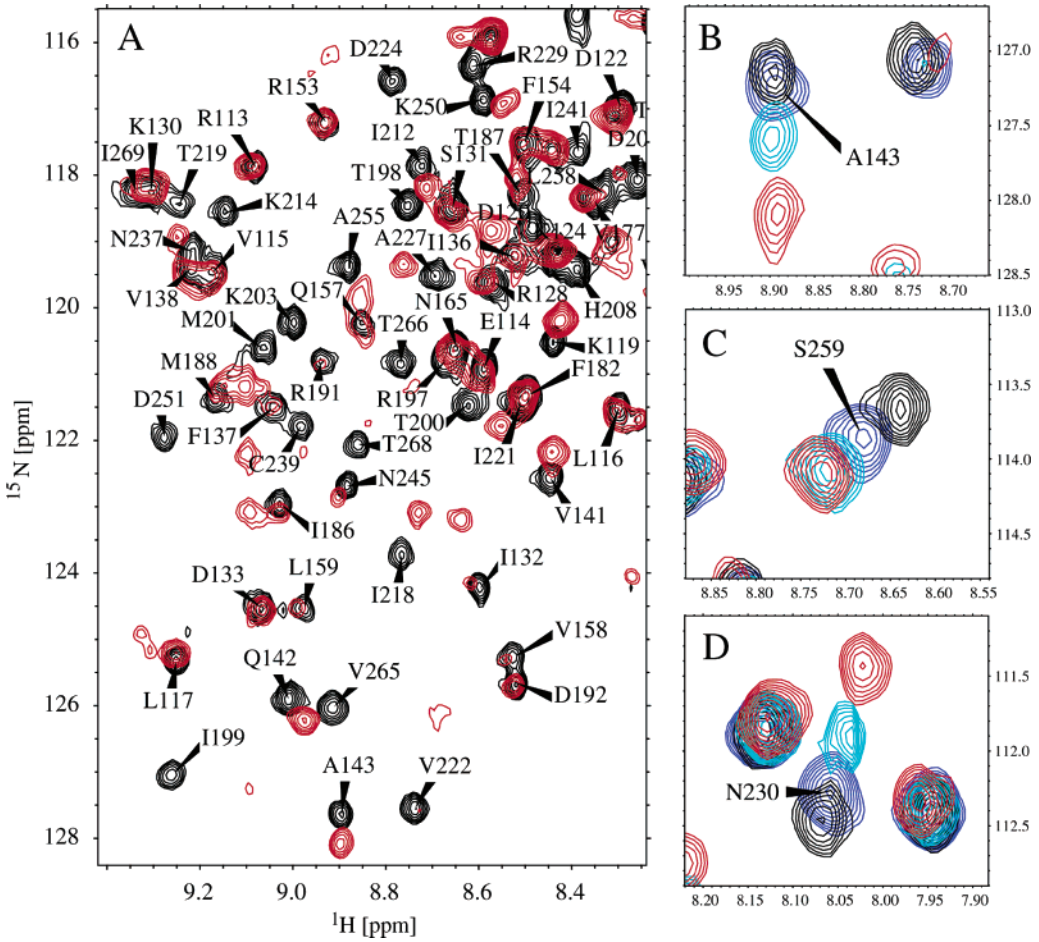

FIGURE 2: Changes in NMR spectra of the syntenin PDZ tandem upon peptide binding. (A) Superposition of the $^{1}H-^{15}N$ HSQC spectra of the free protein (black) and upon addition of TNEFYA at a 1:4 ratio (red). (B−D) Selected fragments of $^{1}H-^{15}N$ HSQC spectra showing different kinetics of chemical shift changes as a function of increasing peptide concentrations: black, free protein; blue, 1:1 ratio; cyan, 1:4 ratio; red, 1:10 ratio. Panels B and C represent titration with TNEFYA, and panel D represents titration with TNEYKV.

Table 2: Dissociation Constants (K_{D1} for the Interactions with PDZ1, K_{D2} for the Interactions with PDZ2) for the Hexapeptides Obtained by NMR Titration

peptide	K_{D1} [mM] NMR	K_{D2} [mM] NMR
TNEFYA	7.6 ± 1.6	0.16 ± 0.01
TNEFYF	1.00 ± 0.07	0.79 ± 0.03
TNEYYV	0.74 ± 0.05	0.10 ± 0.01
TNEYKV	>10	1.15 ± 0.09

Interactions of Peptides with the PDZ2 Domain. Structures of all complexes revealed the presence of the respective peptides in the binding pockets of both PDZ2 domains within the noncrystallographic dimer. All these peptides are inserted into the binding site in an extended conformation and form a β strand which is antiparallel to the β2 strand of PDZ2, as predicted by the canonical model. In all cases the five C-terminal residues are highly ordered and the corresponding electron density is clearly resolved (Figure 3B−D). Due to the lower quality of diffraction data for the complex of syntenin with the syndecan-derived heptadecameric peptide, we did not use these coordinates in subsequent analysis, and instead we used the previously published structure of PDZ2 with the syndecan-derived hexapeptide TNEFYA (1OBY in the PDB).

In general terms, the stabilization of all PDZ2−peptide interactions is achieved through the networks of hydrogen bonds and hydrophobic contacts in a fashion reminiscent of the complex of isolated PDZ2 and the syndecan-derived hexapeptide previously reported by us (*18*). In all cases the main chain of the peptide forms a set of hydrogen bonds with the backbone of the β2 strand of PDZ2. The C-terminal carboxyl groups of all peptides interact with the main chain amides of Val209, Gly210, and Phe211 within the carboxylate-binding loop, a fingerprint motif of PDZ domains. The main chain amide of P_0 is involved in a hydrogen bond with the carbonyl oxygen of Phe211. Additional backbone−backbone hydrogen bonds are formed between residue P_{-2} and Phe213 of PDZ2. The side chains of the residues in P_0, P_{-1}, and P_{-2} positions interact with a number of amino acids lining the corresponding S_0, S_{-1}, and S_{-2} binding pockets. The S_{-3} pocket of PDZ2 is poorly defined and mostly solvent accessible. Consequently, the side chain of Glu at P_{-3} is free to form the critical crystal contact with Arg128 from the symmetry related molecule, thus making it possible to obtain this series of crystalline complexes. The residues upstream of P_{-3} are solvent exposed and not involved in the interactions with PDZ2.

The crystallographic data are fully consistent with the chemical shift changes observed in NMR titration experiments. The most significant changes are traced to those amides which are involved in direct hydrogen bonds with peptides. These include amides forming the carboxylate

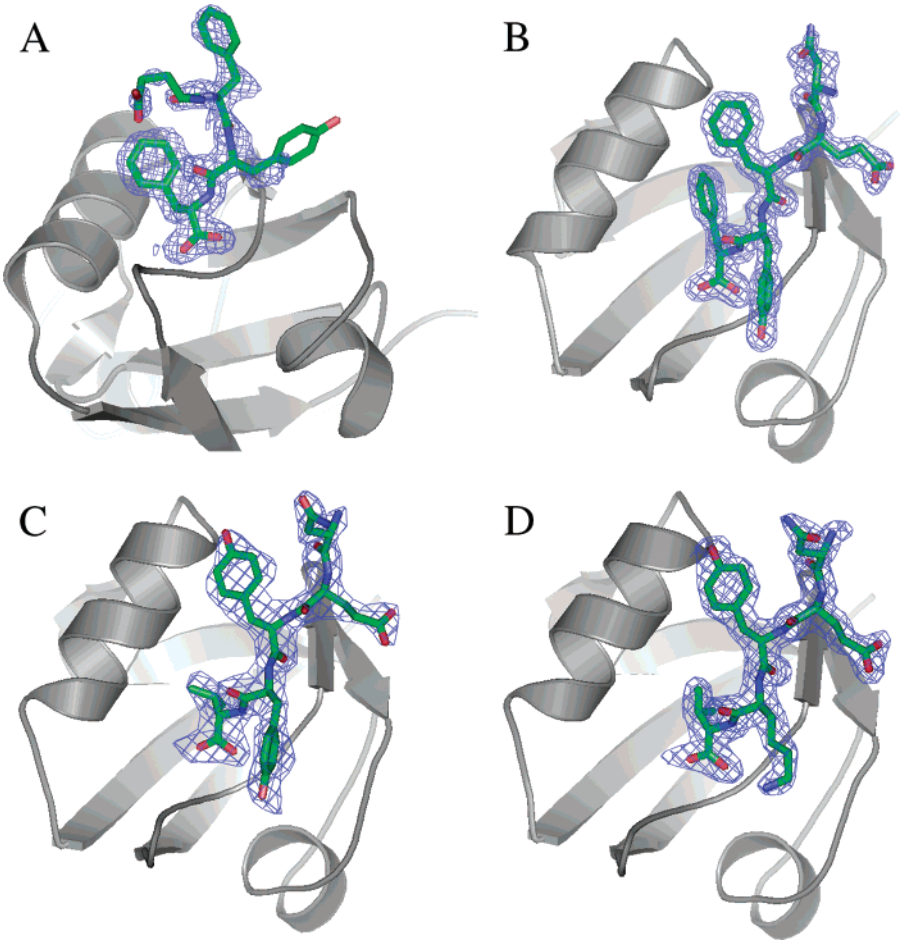

FIGURE 3: A $2mF_o - DF_c$ electron density maps contoured at 1σ for the peptides interacting with syntenin: (A) TNEFYF and PDZ1; (B) TNEFYF and PDZ2; (C) TNEYYV and PDZ2; (D) TNEYKV and PDZ2. The orientation of the PDZ1 domain is different from that of PDZ2 for better presentation of the peptide electron density.

binding loop, i.e., Gly210 and Phe211 (the amide of Val209 is not visible in $^1H-^{15}N$ HSQC spectrum of syntenin tandem) and the amide of Phe213, which is involved in a hydrogen bond with the P_{-2} residue. Additional regions with strong chemical shift changes correlate very well with the location of the binding pockets accommodating the aromatic rings (Figure 1).

As indicated above, the interactions of all peptides with the PDZ2 domain are similar in magnitude, despite differences in the amino acid sequences of the peptides. The analysis of the X-ray structures of the corresponding complexes helps to rationalize this phenomenon. The replacement of Ala at P_0 in syndecan peptide by Phe (the synthetic sequence TNEFYF) did not significantly improve the binding, contrary to our expectations. Although the extent of hydrophobic contacts within the S_0 pocket is clearly higher for Phe, the binding pocket must undergo structural rearrangements which, we believe, are energetically unfavorable (see below). A similar situation is observed upon incorporation of Val at the P_0 position with simultaneous replacement at P_{-2} of Phe by Tyr (TNEYYV peptide). The hydroxyl group of Tyr at P_{-2} is solvent exposed and does not interact with the protein. In contrast, the replacement of Tyr at P_{-1} position by Lys (TNEYKV) decreases the binding several-fold, most likely due to a decrease in hydrophobic contacts and lack of favorable interactions with the side chain amine group. In all peptides, including syndecan derived peptide, the residue P_{-3} and those upstream of it do not contact with the PDZ2 domain. This finding justifies the use of the designed hexapeptides as good models for ephrin and neurexin C-termini.

Induced Fit in PDZ2. The structures reported here along with the previously reported structure of the PDZ2 domain of syntenin with syndecan peptide (*18*) and that of the unliganded syntenin tandem (PDB code 1N99) offer a unique opportunity to investigate an induced fit mechanism in the PDZ2 domain. A least-squares superposition of all models on the core secondary structure elements (excluding the α_2 helix and the β_2 strand which form the binding groove) reveals that the binding of peptides is associated with conformational changes involving a reorientation of the α_2 helix, the residues of which line the S_0 and S_{-2} pockets (Figure 4). In contrast, the β_2 strand appears unaffected.

The most significant structural reorganization affects both the backbone and side chains of residues Asp251 through to Gly262 which belong to the α_2 helix and to the loop that follows (Figure 4). The binding of peptides shifts the α_2 helix apart from the β_2 strand, and the magnitude of this shift depends on the peptide's sequence, and specifically on the size of the P_0 side chain. The smallest shift is observed for syndecan, which has the least bulky side chain, i.e. Ala, at the P_0 position of this peptide. In this case, the α_2 helix moves by approximately 0.5 Å in the region of the S_0 pocket. In the complexes involving neurexin and the ephrin B derived

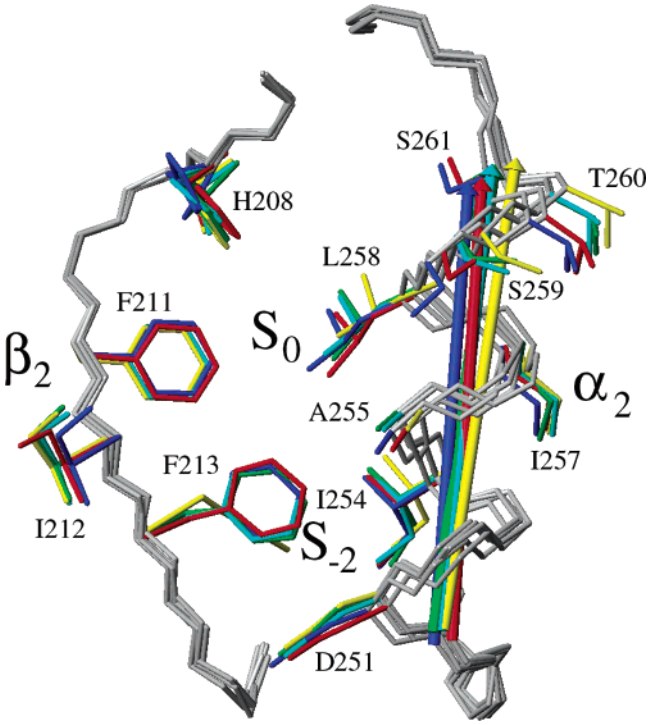

FIGURE 4: Conformational changes in the PDZ2 binding site of syntenin and reorientation of the α_2 helix upon peptide binding. Backbones of β_2 strands and α_2 helices are shown in gray. The side chains of residues in the unliganded syntenin PDZ tandem are in blue (PDB code 1N99); those in the PDZ2−TNEFYA complex are in red (PDB code 1OBY); those of the PDZ tandem with TNEYKV in cyan; those with TNEYYV in green and those with TNEFYF in yellow. Reorientation of the α_2 helices is represented by colored arrows.

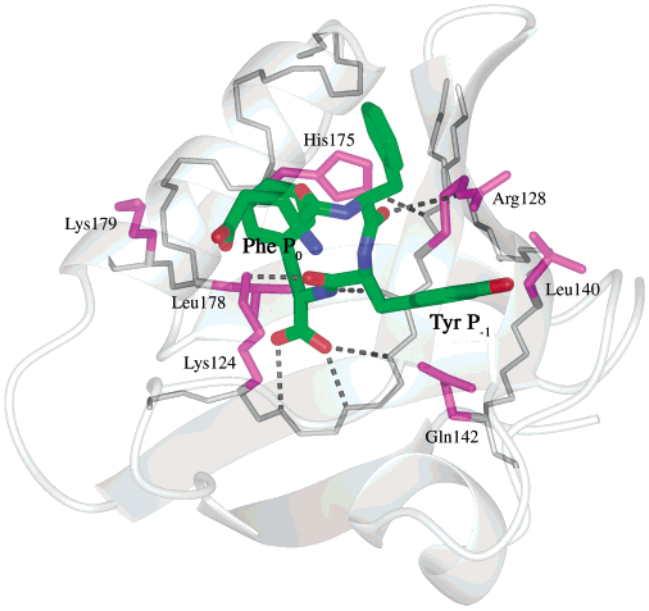

FIGURE 5: Structural details of the interaction of the TNEFYF peptide with syntenin PDZ1. The peptide is shown with green carbon atoms, red oxygens, and blue nitrogens. Side chains of PDZ1 residues involved in the interaction with the peptide are shown in magenta, and intermolecular hydrogen bonds are shown as dashed lines. Note the intramolecular hydrogen bond between Nϵ2 of His175 and the backbone amide of Leu129.

peptides, both of which contain Val at the P_0 position, the shift of the α_2 helix is about 1 Å and in addition the helix rotates around its axis (i.e. rolls) by about 6°. Finally, in the complex with the TNEFYF peptide, the α_2 helix rolls by 6° and is shifted by as much as 1.5 Å. Looking at individual residues, the biggest shift occurs for Leu258, lining the S_0 pocket, whose movement is required to accommodate more bulky residues at the P_0 position. In the complexes with the neurexin and the ephrin peptides, this residue moves by approximately 1 Å, while in the complex with the TNEFYF peptide it is displaced by about 1.5 Å. In addition a large shift of up to 2 Å is observed for residues from Ser259 to Gly262 (Figure 4). This change also contributes to the enlargement of the S_0 pocket and appears to play an important role in the conformational adaptation of the α_2 helix. In the complex of PDZ2 with the syndecan peptide the corresponding loop has an orientation very similar to that observed for the free protein.

By comparison, the fragment of the α_2 helix involved in the formation of the S_{-2} pocket (residues 251−254) is less perturbed. The extent of these changes is similar in all complexes (0.6−0.8 Å), when compared to the unliganded structure. The remaining residues of the S_{-2} binding pocket are not visibly affected. The TNEFYF peptide complex is an exception in that we see a substantial conformational change of the Phe213 side chain at the S_{-2} pocket.

Evidence of Noncanonical Mode of Interaction in the PDZ1 Domain. Interactions mediated by syntenin's PDZ1 domain are less well understood, and to date there are no structural data for any complex with a target peptide and/or protein. Somewhat surprisingly, our NMR data shows that in solution all studied peptides interact with the PDZ1 domain (Figure 1). The X-ray structure of the complex of the PDZ tandem with the TNEFYF peptide reveals clearly resolved electron density corresponding to four C-terminal residues of the peptide in the binding groove of PDZ1 (Figure 3A). The conformation of this peptide represents a unique, noncanonical binding mode. Unlike the canonical interaction, the bound peptide's backbone in PDZ1 is nearly perpendicular to that expected for the canonical binding mode (Figure 5). Only the P_0 and P_{-1} residues of the TNEFYF peptide fit into the corresponding S_0 and S_{-1} pockets, while the remaining part of the peptide is mostly solvent exposed. The anchoring C-terminus binds in a typical fashion in the carboxylate-binding loop consisting of the amides of Ile125, Gly126, and Leu127 (Figure 5). In addition, the carboxyl group is involved in an indirect interaction with the carbonyl group of Gly123 through an ordered water molecule. Hydrogen bonds are also formed between the main chain amide group of the P_0 residue and the carbonyl group of Leu127, and between the carbonyl oxygen of the P_{-1} residue and the side chain amine of Lys124. The Phe side chain at the P_0 position fits well into the S_0 binding pocket formed by His175, Leu178, and Lys179. Moreover, the Phe side chain is involved in a favorable π−cation interaction with Lys124.

The tyrosine at the P_{-1} position of the peptide fits between the side chains of Gln142 and Leu140, which form the S_{-1} pocket. Upstream of the P_{-1} residue, the TNEFYF peptide is solvent exposed. There is only one hydrogen bond formed by the carbonyl group of the P_{-2} residue and the side chain of Arg128. The Phe side chain at P_{-2} does not interact with the PDZ1, but it is engaged in the crystal contacts with Ile212, Val222, and the peptide of the symmetry related

molecule. The glutamate at P_{-3} is totally exposed to water, and its carboxyl group is directed toward Lys179 and Lys124 forming two hydrogen bonds with their side chain amine groups through an ordered water molecule. The P_{-4} and P_{-5} residues have no interpretable electron density.

The noncanonical interaction involving the PDZ1 domain can be rationalized when one considers the differences between the atomic models of the two PDZ domains. While PDZ2 has a broad peptide binding groove exposing β_2 strand which is able to form the antiparallel β structure with the bound peptide, in the case of PDZ1 the translation of the α_2 helix toward β_2 strand by about 3 Å abrogates such stereochemistry (see Figure S1, Suppporting Information). In addition, the side chain of His175 in PDZ1 (Ala in PDZ2) is involved in a hydrogen bond with backbone amide of Leu129 from the β_2 strand, effectively blocking part of the binding pocket and preventing canonical binding (Figure 2S, Supporting Information).

In order to confirm that the noncanonical binding mode of TNEFYF peptide is not an artifact due to crystal packing, we carried out a careful analysis of chemical shift perturbations in solution. As expected, the strongest chemical shift changes for the PDZ1 domain are observed for amides of Ile125, Gly126, and Leu127, which form hydrogen bonds with the C-terminal carboxyl group of the peptide (Figure 2S). However, there are no significant perturbations within the β_2 strand downstream of Arg128 that would be consistent with formation of the antiparallel β sheet with the peptide (see Figure S2). Positions of the S_0 and S_{-1} binding pockets are clearly reflected in chemical shift changes. Binding of the aromatic side chain of Phe in P_0 position causes chemical shift perturbations for the α_2 helix residues: His175, Lys176, Val177, Lys179, and Gln180, while the Tyr in P_{-1} site affects chemical shifts of Arg128 (β_2), Leu140 and Val141 (β_3), and Gln142 and Ala143 (loop connecting β_3 and β_4). The residues upstream of P_{-1} (except for P_{-2} backbone carbonyl) do not contact the PDZ1 domain and do not cause additional chemical shift changes. In summary, the observed pattern of chemical shift perturbations is fully consistent with the noncanonical binding of TNEFYF seen in the crystal structure of PDZ1.

A very similar pattern of chemical shift changes in solution is also observed upon binding of other peptides to the PDZ1 domain. Although we were unable to obtain a crystal structure of the complex of syndecan peptide bound to PDZ1, we performed detailed comparison of chemical shift changes upon binding of TNEFYA and TNEFYF (see Figure S2A,B). The strongest changes are observed for amides directly hydrogen bonded to the C-terminal carboxylate of both peptides (Figure S2). Because of the presence of Ala residue in the P_0 position of syndecan peptide, chemical shift changes observed in the S_0 pockets are modest. Stronger perturbations are observed in the S_{-1} site due to the presence of the aromatic Tyr side chain. Qualitatively, the overall pattern of chemical shift changes is very similar for both peptides, although a smaller magnitude of perturbations seen for TNEFYA results from weaker interaction. We also obtained very similar results from comparison of TNEFYF and TNEYYV peptides (data not shown). Based on this analysis we conclude that both syndecan and neurexin derived peptides bind to PDZ1 in a noncanonical manner that is comparable to that for the complex with TNEFYF.

DISCUSSION

Although PDZ domains are among the most intensely studied protein modules, the mechanism by which these proteins exert their biological function is still unclear. The canonical model postulates that PDZ domains bind to C-termini of membrane receptors and channels, so that the terminal carboxylates are anchored within a distinct glycine-rich loop, while residues in positions P_0 and P_{-2} serve as specificity determinant. This oversimplified view does not explain the diversity and specificity of PDZ-mediated interactions, and the model was accordingly expanded to include, among others, interactions with internal sequences (*27*, *28*), and binding modes involving residues in the P_{-1} position (*29*−*31*) as well as residues upstream of the terminal tripeptide (*29*, *30*, *32*−*34*). Unfortunately, no generic mechanism appears to apply universally to all PDZ domains, particularly given the possibility of complex cooperative effects between different PDZ domains along the same polypeptide chain, as well as degenerate specificities.

Previous data suggested that syntenin, with its two PDZ domains, shows cooperativity when binding to syndecans, neurexins, and ephrin B. Our NMR titration experiments using peptides corresponding to the C-termini of these three proteins show that all bind to both PDZ domains within an intact tandem, albeit with moderate K_D values in the high μM to mM range. Syndecan-derived peptides were previously reported to bind more tightly (*7*), and to investigate the source of this discrepancy we conducted a series of isothermal calorimetric measurements of all four peptides to the isolated PDZ2 domain (data not shown). The binding constants obtained for syndecan, neurexin, and ephrin B hexapeptides using ITC and NMR titration experiments are within experimental error. While it is not clear why the previously reported binding data (*7*) and those reported here are at variance, our key conclusions that all four peptides bind to both PDZ domains, and that the affinities toward PDZ1 are either comparable or 10-fold lower, are not in dispute.

In our previously published study we showed how the PDZ2 domain can accommodate different sequences of bound peptides, utilizing its three pockets (S_0, S_{-1}, and S_{-2}) in a combinatorial fashion (*7*). This study extends our model by showing that the PDZ2 domain also utilizes induced fit to adapt to different peptide ligands. Although these data are unique with respect to the number of different peptides cocrystallized with a single PDZ domain, there is indication from other studies that an induced fit mechanism might be a more general feature of the C-terminal target recognition by PDZ domains. For example, a reorientation of the α_2 helix, similar to the one described in this paper, was also observed for PDZ6 of GRIP1 (*35*). It is also likely that the plasticity of the PDZ domains may have been generally exploited in the course of evolution to build in regulatory mechanisms. For instance, binding of internal sequences of Pals1 to the single PDZ domain of Par-6 deforms the latter's binding pocket, bypassing the requirement for a free terminal carboxylate (*27*). Since Par-6 also binds to C-terminal ligands in a manner regulated by the GTPase Cdc42, the system allows for complex and competitive regulation that may be important to cell polarity (*27*).

Just as degenerate specificity rationalizes a level of promiscuity of PDZ domains with respect to their targets,

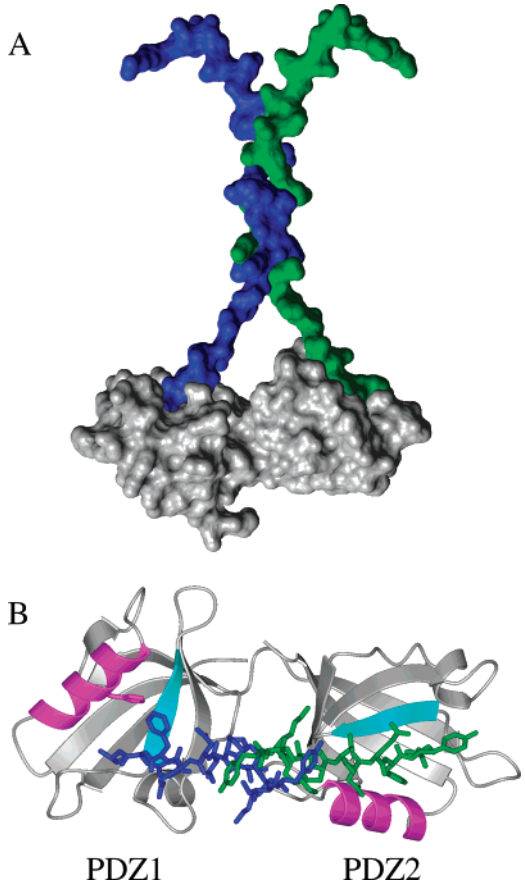

FIGURE 6: A model of the syndecan−syntenin complex obtained by docking of the NMR structure of syndecan dimer (PDB code 1ejp) onto the syntenin PDZ tandem structure from the complex with the TNEFYF peptide. (A) Surface representation of the syntenin tandem molecule (gray) and docked syndecan dimer (green and blue). (B) View from the top showing major difference between canonical interaction in PDZ2 and noncanonical binding to PDZ1. An α_2 helix and β_2 strand forming the canonical binding site are colored in magenta and cyan, respectively. The position of the side chain of His175 is shown in magenta.

cooperativity requires that two comparatively different PDZ domains within one protein bind identical sequences. The crystal structure of the PDZ1 domain of syntenin within the tandem shows that with its narrow binding groove it is unable to accommodate ligands in a normal, extended conformation. The separation between the α_2 helix and the β_2 strand, which flank the binding pocket, is about 2−3 Å shorter in PDZ1 than in the PDZ2 domain (Figure 6B). In addition, the binding site is largely blocked by the side chain of His175 in a conformation stabilized by a hydrogen bond between the unprotonated Nϵ2 of His175 and the backbone amide of Leu129 (Figure 5). This is not an artifact of the crystal structure, because a chemical shift of this amide is significantly perturbed downfield ($\sigma = 11.7$ ppm) indicating that a strong hydrogen bond is present in solution both for free syntenin and in complexes with peptides. In the absence of a canonical binding site, peptides bind to the PDZ1 domain in a different manner, exemplified by the TNEFYF peptide. Although we observe this binding in one crystal structure only, NMR data confirm that in solution other sequences follow the same pattern. A similar binding mode has recently been reported for the autoinhibited conformation of the X11α PDZ tandem (*36*). The NMR-derived structure revealed that the C-terminal tail of X11α inserts into the first PDZ domain in an orientation that is approximately perpendicular to the canonical binding pocket. Similarly to PDZ1 of syntenin, only two C-terminal amino acids of the X11α tail, P_0 and P_{-2}, are directly involved in PDZ1 binding. Another noncanoncal, PDZ−peptide interaction without β-sheet augmentation has also been reported for the PDZ1 domain of NHERF (*37*). In the X-ray structure, the carboxy-terminal sequence of PDZ1 occupies the peptide binding pocket of a neighboring PDZ1 molecule related by crystallographic symmetry. In this example, the P_0 and P_{-2} residues are involved in the interactions with the PDZ domain, while P_{-1} and residues upstream of P_{-2} are exposed to the solvent. Thus, there is now mounting evidence supporting the biological relevance of the noncanonical peptide binding to selected PDZ domains.

Taken together with previous data, our results make it possible to propose a model of a supramolecular complex between the syndecan cytoplasmic domain and syntenin's PDZ tandem. The crystal structure of the syntenin's PDZ tandem shows compact supramodular architecture of the two PDZ domains (*7*). Furthermore, our recent NMR data show that the tandem of PDZ1 and PDZ2 exists as a monomer in solution and tumbles as a single domain (*25*). A rigid relative orientation of the two PDZ domains in syntenin imposes constraints on the relative orientation of the two interacting peptides. This can be exemplified by the structure of syntenin with the TNEFYF peptide. Based on the chemical shift perturbations, we have shown that this binding mode is consistent with the structure in solution. Detailed analysis of NMR data reveals that syndecan peptide also binds to PDZ1 in a very similar, noncanonical mode.

Owing to a noncanonical conformation of the peptide ligand bound to the PDZ1 domain, the two peptides bind in a nearly collinear, antiparallel fashion (Figure 6). As a consequence, the N-termini of the peptides are close to each other. Such mutual disposition of the two peptides corresponds well to that inferred from the dimeric structure of the cytoplasmic domain of syndecan-4, syntenin's physiological ligand (*38*). NMR studies show that the 28 amino acid long cytoplasmic domain of syndecan-4 forms an intertwined dimer with a symmetric clamp shape in its central region and flexible N- and C-termini (*38*). Such a dimeric structure fits perfectly into syntenin's two binding pockets, with one C-terminus interacting in a canonical fashion with PDZ2 and a second interacting with PDZ1 in a binding mode which we see in the complex with the TNEFYF peptide (Figure 6). It is noteworthy that canonical binding to PDZ1 would prevent such interaction.

Multiple PDZ domains are a common feature in many proteins, and at least some of them display distinct supramodular architectures (*39*−*41*). For example, the structure of the PSD-95 PDZ domain tandem reveals a restricted arrangement of PDZ domains leading to a fixed mutual disposition of the bound peptides (*41*). In the case of the Shank protein, a similar biological effect is observed as a result of dimerization of two PDZ modules from two different molecules, facilitating binding to dimeric ligands (*40*). The model of dimeric ligand binding to syntenin, which we propose here, represents a novel supramolecular architecture. Most importantly, it justifies cooperative binding observed for syntenin (*8*, *14*). Furthermore, our results are

in good agreement with previously published data demonstrating that single PDZ domains of syntenin do not provide strong binding of syndecan (*8*, *14*, *15*, *42*). Instead, the two PDZ domains participate cooperatively with PDZ2 being the dominant module. From the thermodynamic point, cooperative binding of the syndecan dimer to syntenin should result in improved binding affinity relative to monomeric ligands, such as a peptide, because the resultant K_D can reach a value equivalent to a product of the individual dissociation constants.

Biological function of the cell surface proteins is frequently related to their oligomerization state. Clustering of the ephrin molecules, which is also a syntenin target, has been found to be relevant to cell−cell recognition and targeting (*43*). The C-terminal region of the cytoplasmic domain of ephrin B adopts a well-packed β-hairpin structure with a flexible tail containing a PDZ recognition motif. Interestingly, the N-terminal fragment of this domain is prone to aggregation and has been proposed to participate in ephrin multimerization (*44*). Our studies of the interaction between the ephrin B derived peptide and syntenin show weak affinity toward PDZ2 and just marginal for PDZ1. This is in good agreement with a previous report indicating that the intact cytoplasmic fragment of ephrin B does not detectably associate with PDZ1 and exhibits weak interaction with PDZ2 (*16*). Strong interactions with ephrin B require both PDZ domains (*14*, *44*). We believe that the oligomeric form of the cytoplasmic fragment of ephrin B will interact with both PDZ1 and PDZ2 domains of syntenin in a manner similar to that which we suggest for syndecan.

Of the peptides investigated in the present study, the neurexin derived hexapeptide is the most potent ligand toward both PDZ1 and PDZ2 domains. This is consistent with other data that show that PDZ1 has a higher intrinsic affinity toward neurexins than toward syndecans and ephrin B (*14*). The modular architecture of neurexins is similar to that of syndecans and ephrins B, including the presence of a short cytoplasmic fragment containing a C-terminal motif recognized by the PDZ domains (*45*). Although we are not aware of any data indicating neurexin dimerization, it was shown that syntenin binds neurexins using synergistically both PDZ domains (*14*, *15*). Therefore, it is highly possible that our model may also extend to neurexins.

The common feature emerging from our experiments is that syntenin binds ligands with weaker affinities than typically observed 1−10 μM for other PDZ domains (*2*). Although very weak protein−protein interactions are far more difficult to characterize, they may play an important role in many biological processes (*46*). The relatively weak interactions of syntenin with monomeric peptides suggests that syntenin has evolved to bind preferably to specific oligomeric structures rather than to promote protein assembly.

ACKNOWLEDGMENT

We thank Dr. David Cooper for help with the refinement and Dr. Zbigniew Dauter for help with data collection at NSLS. We also thank the staff of the Southeastern Region Collaborative Access Team (SER-CAT) at the Advanced Photon Source, Argonne National Laboratory, for their help. Use of the APS was supported by the U.S. Department of Energy, Office of Science, Office of Basic Energy Sciences, under Contract No. W-31-109-Eng-38.

SUPPORTING INFORMATION AVAILABLE

Figure S1, presenting the structural differences between the PDZ1 and PDZ2 domains of syntenin and their interactions with peptides, and Figure S2, showing a detailed comparison of chemical shift changes upon titration of syntenin PDZ domains with peptides. This material is available free of charge via the Internet at http://pubs.acs.org.

REFERENCES

1. Fan, J. S., and Zhang, M. (2002) Signaling complex organization by PDZ domain proteins, *Neurosignals 11*, 315−21.
2. Nourry, C., Grant, S. G., and Borg, J. P. (2003) PDZ domain proteins: plug and play!, *Sci. STKE 2003*, RE7.
3. Sheng, M., and Sala, C. (2001) PDZ domains and the organization of supramolecular complexes, *Annu. Rev. Neurosci. 24*, 1−29.
4. Zhang, M., and Wang, W. (2003) Organization of signaling complexes by PDZ-domain scaffold proteins, *Acc. Chem. Res. 36*, 530−8.
5. Bezprozvanny, I., and Maximov, A. (2001) Classification of PDZ domains, *FEBS Lett. 509*, 457−62.
6. Vaccaro, P., and Dente, L. (2002) PDZ domains: troubles in classification, *FEBS Lett 512*, 345−9.
7. Kang, B. S., Cooper, D. R., Jelen, F., Devedjiev, Y., Derewenda, U., Dauter, Z., Otlewski, J., and Derewenda, Z. S. (2003) PDZ tandem of human syntenin: crystal structure and functional properties, *Structure (Cambridge) 11*, 459−68.
8. Grootjans, J. J., Zimmermann, P., Reekmans, G., Smets, A., Degeest, G., Durr, J., and David, G. (1997) Syntenin, a PDZ protein that binds syndecan cytoplasmic domains, *Proc. Natl. Acad. Sci. U.S.A. 94*, 13683−8.
9. Zimmermann, P., Tomatis, D., Rosas, M., Grootjans, J., Leenaerts, I., Degeest, G., Reekmans, G., Coomans, C., and David, G. (2001) Characterization of syntenin, a syndecan-binding PDZ protein, as a component of cell adhesion sites and microfilaments, *Mol. Biol. Cell 12*, 339−50.
10. Fernandez-Larrea, J., Merlos-Suarez, A., Urena, J. M., Baselga, J., and Arribas, J. (1999) A role for a PDZ protein in the early secretory pathway for the targeting of proTGF-alpha to the cell surface, *Mol. Cell 3*, 423−33.
11. Fialka, I., Steinlein, P., Ahorn, H., Bock, G., Burbelo, P. D., Haberfellner, M., Lottspeich, F., Paiha, K., Pasquali, C., and Huber, L. A. (1999) Identification of syntenin as a protein of the apical early endocytic compartment in Madin-Darby canine kidney cells, *J. Biol. Chem. 274*, 26233−9.
12. Geijsen, N., Uings, I. J., Pals, C., Armstrong, J., McKinnon, M., Raaijmakers, J. A., Lammers, J. W., Koenderman, L., and Coffer, P. J. (2001) Cytokine-specific transcriptional regulation through an IL-5Ralpha interacting protein, *Science 293*, 1136−8.
13. Koo, T. H., Lee, J. J., Kim, E. M., Kim, K. W., Kim, H. D., and Lee, J. H. (2002) Syntenin is overexpressed and promotes cell migration in metastatic human breast and gastric cancer cell lines, *Oncogene 21*, 4080−8.
14. Grootjans, J. J., Reekmans, G., Ceulemans, H., and David, G. (2000) Syntenin-syndecan binding requires syndecan-synteny and the co-operation of both PDZ domains of syntenin, *J. Biol. Chem. 275*, 19933−41.
15. Koroll, M., Rathjen, F. G., and Volkmer, H. (2001) The neural cell recognition molecule neurofascin interacts with syntenin-1 but not with syntenin-2, both of which reveal self-associating activity, *J. Biol. Chem. 276*, 10646−54.
16. Lin, D., Gish, G. D., Songyang, Z., and Pawson, T. (1999) The carboxyl terminus of B class ephrins constitutes a PDZ domain binding motif, *J. Biol. Chem. 274*, 3726−33.
17. Torres, R., Firestein, B. L., Dong, H., Staudinger, J., Olson, E. N., Huganir, R. L., Bredt, D. S., Gale, N. W., and Yancopoulos, G. D. (1998) PDZ proteins bind, cluster, and synaptically colocalize with Eph receptors and their ephrin ligands, *Neuron 21*, 1453−63.
18. Kang, B. S., Cooper, D. R., Devedjiev, Y., Derewenda, U., and Derewenda, Z. S. (2003) Molecular roots of degenerate specificity in syntenin's PDZ2 domain: reassessment of the PDZ recognition paradigm, *Structure (Cambridge) 11*, 845−53.

19. Otwinowski, Z., and Minor, W. (1997) Processing of X-ray diffraction data collected in oscillation mode, *Methods Enzymol. 276*, 307−26.
20. Navaza, J. (1994) AMoRe: an automated package for molecular replacement, *Acta Crystallogr. A 50*, 157−63.
21. Murshudov, G. N. (1997) Refinement of macromolecular structures by the maximum-likelihood method, *Acta Crystallogr., D: Biol. Crystallogr. 53*, 240−55.
22. CCP4 (Collaborative Computational Project Number 4) (1994) The CCP4 suite: programs for protein crystallography, *Acta Crystallogr., D: Biol. Crystallogr. 50*, 760−3.
23. Jones, T. A., Zou, J.-Y., Cowan, S. W., and Kjeldgaard, M. (1991) Improved methods for building protein models in electron density maps and the location of errors in these models, *Acta Crystallogr. A 47*, 110−19.
24. Johnson, P. E., Tomme, P., Joshi, M. D., and McIntosh, L. P. (1996) Interaction of soluble cellooligosaccharides with the N-terminal cellulose-binding domain of Cellulomonas fimi CenC 2. NMR and ultraviolet absorption spectroscopy, *Biochemistry 35*, 13895−906.
25. Cierpicki, T., Bushweller, J. H., and Derewenda, Z. S. (2005) Probing the supramodular architecture of a multidomain protein: the structure of syntenin in solution, *Structure (Cambridge) 13*, 319−27.
26. Delaglio, F., Grzesiek, S., Vuister, G. W., Zhu, G., Pfeifer, J., and Bax, A. (1995) NMRPipe: a multidimensional spectral processing system based on UNIX pipes, *J. Biomol. NMR 6*, 277−93.
27. Penkert, R. R., DiVittorio, H. M., and Prehoda, K. E. (2004) Internal recognition through PDZ domain plasticity in the Par-6-Pals1 complex, *Nat. Struct. Mol. Biol. 11*, 1122−7.
28. Hillier, B. J., Christopherson, K. S., Prehoda, K. E., Bredt, D. S., and Lim, W. A. (1999) Unexpected modes of PDZ domain scaffolding revealed by structure of nNOS-syntrophin complex, *Science 284*, 812−5.
29. Niethammer, M., Valtschanoff, J. G., Kapoor, T. M., Allison, D. W., Weinberg, T. M., Craig, A. M., and Sheng, M. (1998) CRIPT, a novel postsynaptic protein that binds to the third PDZ domain of PSD-95/SAP90, *Neuron 20*, 693−707.
30. Songyang, Z., Fanning, A. S., Fu, C., Xu, J., Marfatia, S. M., Chishti, A. H., Crompton, A., Chan, A. C., Anderson, J. M., and Cantley, L. C. (1997) Recognition of unique carboxyl-terminal motifs by distinct PDZ domains, *Science 275*, 73−7.
31. Stricker, N. L., Christopherson, K. S., Yi, B. A., Schatz, P. J., Raab, R. W., Dawes, G., Bassett, D. E., Jr., Bredt, D. S., and Li, M. (1997) PDZ domain of neuronal nitric oxide synthase recognizes novel C-terminal peptide sequences, *Nat. Biotechnol. 15*, 336−42.
32. Kozlov, G., Gehring, K., and Ekiel, I. (2000) Solution structure of the PDZ2 domain from human phosphatase hPTP1E and its interactions with C-terminal peptides from the Fas receptor, *Biochemistry 39*, 2572−80.
33. Skelton, N. J., Koehler, M. F., Zobel, K., Wong, W. L., Yeh, S., Pisabarro, M. T., Yin, J. P., Lasky, L. A., and Sidhu, S. S. (2003) Origins of PDZ domain ligand specificity. Structure determination and mutagenesis of the Erbin PDZ domain, *J. Biol. Chem. 278*, 7645−54.
34. Birrane, G., Chung, J., and Ladias, J. A. (2003) Novel mode of ligand recognition by the Erbin PDZ domain, *J. Biol. Chem. 278*, 1399−402.
35. Im, Y. J., Park, S. H., Rho, S. H., Lee, J. H., Kang, G. B., Sheng, M., Kim, E., and Eom, S. H. (2003) Crystal structure of GRIP1 PDZ6-peptide complex reveals the structural basis for class II PDZ target recognition and PDZ domain-mediated multimerization, *J. Biol. Chem. 278*, 8501−7.
36. Long, J. F., Feng, W., Wang, R., Chan, L. N., Ip, F. C., Xia, J., Ip, N. Y., and Zhang, M. (2005) Autoinhibition of X11/Mint scaffold proteins revealed by the closed conformation of the PDZ tandem, *Nat. Struct. Mol. Biol. 12*, 722−8.
37. Karthikeyan, S., Leung, T., Birrane, G., Webster, G., and Ladias, J. A. (2001) Crystal structure of the PDZ1 domain of human Na-(+)/H(+) exchanger regulatory factor provides insights into the mechanism of carboxyl-terminal leucine recognition by class I PDZ domains, *J. Mol. Biol. 308*, 963−73.
38. Shin, J., Lee, W., Lee, D., Koo, B. K., Han, I., Lim, Y., Woods, A., Couchman, J. R., and Oh, E. S. (2001) Solution structure of the dimeric cytoplasmic domain of syndecan-4, *Biochemistry 40*, 8471−8.
39. Feng, W., Shi, Y., Li, M., and Zhang, M. (2003) Tandem PDZ repeats in glutamate receptor-interacting proteins have a novel mode of PDZ domain-mediated target binding, *Nat. Struct. Biol. 10*, 972−8.
40. Im, Y. J., Lee, J. H., Park, S. H., Park, S. J., Rho, S. H., Kang, G. B., Kim, E., and Eom, S. H. (2003) Crystal structure of the Shank PDZ-ligand complex reveals a class I PDZ interaction and a novel PDZ-PDZ dimerization, *J. Biol. Chem. 278*, 48099−104.
41. Long, J. F., Tochio, H., Wang, P., Fan, J. S., Sala, C., Niethammer, M., Sheng, M., and Zhang, M. (2003) Supramodular structure and synergistic target binding of the N-terminal tandem PDZ domains of PSD-95, *J. Mol. Biol. 327*, 203−14.
42. Bass, M. D., and Humphries, M. J. (2002) Cytoplasmic interactions of syndecan-4 orchestrate adhesion receptor and growth factor receptor signalling, *Biochem. J. 368*, 1−15.
43. Stein, E., Lane, A. A., Cerretti, D. P., Schoecklmann, H. O., Schroff, A. D., Van Etten, R. L., and Daniel, T. O. (1998) Eph receptors discriminate specific ligand oligomers to determine alternative signaling complexes, attachment, and assembly responses, *Genes Dev. 12*, 667−78.
44. Song, J., Vranken, W., Xu, P., Gingras, R., Noyce, R. S., Yu, Z., Shen, S. H., and Ni, F. (2002) Solution structure and backbone dynamics of the functional cytoplasmic subdomain of human ephrin B2, a cell-surface ligand with bidirectional signaling properties, *Biochemistry 41*, 10942−9.
45. Missler, M., Fernandez-Chacon, R., and Sudhof, T. C. (1998) The making of neurexins, *J. Neurochem. 71*, 1339−47.
46. Vaynberg, J., Fukuda, T., Chen, K., Vinogradova, O., Velyvis, A., Tu, Y., Ng, L., Wu, C., and Qin, J. (2005) Structure of an ultraweak protein-protein complex and its crucial role in regulation of cell morphology and motility, *Mol. Cell 17*, 513−23.

BI052225Y